



ELSEVIER

Contents lists available at ScienceDirect

European Journal of Pharmacology

journal homepage: www.elsevier.com/locate/ejphar

Neuropharmacology and analgesia

Neuroprotective effects of rosuvastatin against traumatic spinal cord injury in rats



Ramazan Kahveci^a, Emre Cemal Gökçe^b, Bora Güre^{c,*}, Aysun Gökçe^d, Uçler Kisa^e, Duran Berker Cemil^b, Mustafa Fevzi Sargon^f, Fatih Ozan Kahveci^g, Nurkan Aksoy^e, Bülent Erdoğan^b

^a Ministry of Health, Kirikkale Yüksek İhtisas Hospital, Department of Neurosurgery, Kirikkale, Turkey

^b Turgut Ozal University, Faculty of Medicine, Department of Neurosurgery, Ankara, Turkey

^c Ministry of Health, Fatih Sultan Mehmet Education and Research Hospital, Department of Neurosurgery, Beyin Cerrahi Servisi, 34752 Ataşehir, Istanbul, Turkey

^d Ministry of Health, Diskapi Yıldırım Beyazıt Education and Research Hospital, Department of Pathology, Ankara, Turkey

^e Kirikkale University, Faculty of Medicine, Department of Biochemistry, Kirikkale, Turkey

^f Hacettepe University, Faculty of Medicine, Department of Anatomy, Ankara, Turkey

^g Bülent Ecevit University, Faculty of Medicine, Department of Emergency Medicine, Zonguldak, Turkey

ARTICLE INFO

Article history:

Received 25 January 2014

Received in revised form

18 July 2014

Accepted 21 July 2014

Available online 29 July 2014

Keywords:

Methylprednisolone

Neuroprotection

Rat

Rosuvastatin

Spinal cord injury

Trauma

ABSTRACT

Rosuvastatin, which is a potent statin, has never been studied in traumatic spinal cord injury. The aim of this study was to investigate whether rosuvastatin treatment could protect the spinal cord after experimental spinal cord injury. Rats were randomized into the following five groups of eight animals each: control, sham, trauma, rosuvastatin, and methylprednisolone. In the control group, no surgical intervention was performed. In the sham group, only laminectomy was performed. In all the other groups, the spinal cord trauma model was created by the occlusion of the spinal cord with an aneurysm clip. In the spinal cord tissue, caspase-3 activity, tumor necrosis factor-alpha levels, myeloperoxidase activity, malondialdehyde levels, nitric oxide levels, and superoxide dismutase levels were analyzed. Histopathological and ultrastructural evaluations were also performed. Neurological evaluation was performed using the Basso, Beattie, and Bresnahan locomotor scale and the inclined-plane test. After traumatic spinal cord injury, increases in caspase-3 activity, tumor necrosis factor-alpha levels, myeloperoxidase activity, malondialdehyde levels, and nitric oxide levels were detected. In contrast, the superoxide dismutase levels were decreased. After the administration of rosuvastatin, decreases were observed in the tissue caspase-3 activity, tumor necrosis factor-alpha levels, myeloperoxidase activity, malondialdehyde levels, and nitric oxide levels. In contrast, tissue superoxide dismutase levels were increased. Furthermore, rosuvastatin treatment showed improved results concerning the histopathological scores, the ultrastructural score and the functional tests. Biochemical, histopathological, ultrastructural analysis and functional tests revealed that rosuvastatin exhibits meaningful neuroprotective effects against spinal cord injury.

© 2014 Elsevier B.V. All rights reserved.

1. Introduction

Spinal cord injury (SCI) causes catastrophic neurological consequences that often conclude with irreversible neurological deficits. The spinal cord is first exposed to the initial physical impact, which is called the primary injury. Following the primary injury, several pathways activate the secondary injury causing the death of additional neuronal tissues (Dumont et al., 2001; Mautes et al., 2000). In

particular, the secondary damage is determined by numerous cellular, molecular and biochemical pathways, but the exact pathophysiological mechanisms are still unknown (Blight, 1992), although inflammation, formation of reactive oxygen species, lipid peroxidation, and apoptosis are known to play important roles (Cemil et al., 2010; Crowe et al., 1997; Esposito et al., 2012; Liu et al., 1997; Pannu et al., 2005; Vaziri et al., 2004).

Statins, structural analogs of 3-hydroxy-3-methylglutaryl coenzyme A (HMG-CoA) reductase, are currently used for the treatment of hyperlipidemia and the prevention of cardiovascular disease (Fletcher et al., 2005). In addition to the anti-lipidemic effects, other possible beneficial effects such as neuroprotection

* Corresponding author. Tel.: +90 506 316 42 01; fax: +90 216 578 30 00.

E-mail address: boragurer@gmail.com (B. Güre).

have been suggested (Laufs et al., 2002; Stepień et al., 2005; Vaughan and Delanty, 1999). Simvastatin and atorvastatin had been widely investigated in traumatic SCI and have been found to be neuroprotective (Déry et al., 2009; Esposito et al., 2012; Han et al., 2012, 2011; Mann et al., 2010; Pannu et al., 2007, 2005).

Rosuvastatin (ROS), a relatively new HMG-CoA reductase inhibitor has exhibited more potent affinity for HMG-CoA reductase and has the longest terminal half-life compared to the other statins (McTaggart et al., 2001). Previously, ROS had been found to have neuroprotective effects against spinal cord ischemia/reperfusion injury (Die et al., 2010; Ucak et al., 2011; Yavuz et al., 2013), ischemic brain injury (Kilic et al., 2005; Prinz et al., 2008; Savoia et al., 2011), traumatic brain injury (Indraswari et al., 2012; Jungner et al., 2013; Sánchez-Aguilar et al., 2013), and L-glutamate induced excitotoxicity (Domoki et al., 2010). However, the effects of ROS in experimental traumatic SCI have not been investigated.

The aim of this study was to investigate whether ROS treatment protects the spinal cord from apoptosis, inflammation, and oxidative stress in rats after experimental traumatic SCI. We also compared ROS with methylprednisolone (MP), which has been widely researched in traumatic SCI.

2. Materials and methods

2.1. Experimental groups

Animal care and all experiments were in compliance with the European Communities Council Directive of November 24, 1986 (86/609/EEC) on the protection of animals for experimental use. All experimental procedures used in this investigation were reviewed and approved by the ethical committee of the Ministry of Health Ankara Education and Research Hospital. Forty adult male Wistar Albino rats weighing 250 ± 20 g were used. The rats were randomly assigned to five groups with eight rats per group. The groups were as follows:

Group 1: control ($n=8$); no surgical procedure was performed. Non-traumatized spinal cord samples were obtained from the control group to determine normal spinal cord morphology and baseline biochemical values.

Group 2: sham ($n=8$); rats underwent only a simple laminectomy. Non-traumatized spinal cord samples were removed after 24 h.

Group 3: trauma ($n=8$); rats underwent SCI as described below. After laminectomy, spinal cord samples were removed 24 h post-injury. Rats received a single intraperitoneal dose of 1 cc physiological saline (0.9% NaCl) as vehicle.

Group 4: rosuvastatin (ROS) ($n=8$); similar to group 3, but rats received a single intraperitoneal dose of 20 mg/kg ROS (AstraZeneca, Cheshire, United Kingdom) immediately following SCI.

Group 5: methylprednisolone (MP) ($n=8$); similar to group 3, but rats received a single intraperitoneal dose of 30 mg/kg MP (Prednol, Mustafa Nevzat, Turkey) immediately following SCI.

2.2. Anesthesia and spinal cord injury procedure

All rats were kept under environmentally controlled conditions at 22–25 °C, with appropriate humidity and a 12-h light cycle and granted free access to food and water.

The animals were anesthetized with an intraperitoneal injection of 10 mg/kg xylazine (Rompun, Bayer, Turkey) and 50 mg/kg ketamine (Ketalar, Parke Davis, Turkey), and allowed to breathe spontaneously. A rectal probe was inserted, and the animals were positioned on a heating pad that maintained the body temperature at 37 °C.

The rats were placed in a prone position. A T5 through T9 midline skin incision was made, and the paravertebral muscles were dissected. From T6 to T8, the spinous processes were removed, and laminectomy was performed. The dura was left intact. An aneurysm clip of 70 g closing force (Yasargil FE 721, Aesculap, Germany) was applied to the T7 level of the spinal cord for 1 min (Cemil et al., 2010; Kurt et al., 2009). At the end of the procedure, the clip was removed, and the surgical wound was closed in layers with silk sutures. The drugs were administered intraperitoneally immediately after the wound was closed. The animals were killed 24 h after the operation by injection of high-dose (200 mg/kg) pentobarbital (Nembutal, Oak Pharmaceuticals, Lake Forest, IL, USA); then spinal cord samples (15 mm) were obtained from the operated area and divided into three equal parts. Cranial parts of the tissue samples were used for light microscopic evaluation, the middle parts were used for electron microscopic evaluation and the caudal parts were cleared of blood with a scalpel and immediately stored at -80 °C for biochemical analysis.

2.3. Biochemical procedures

For the analysis, the tissues were homogenized in physiologic saline solution and centrifuged at 4000g for 20 min. Then, the upper clear supernatants were removed for the analysis.

2.3.1. Tissue caspase-3 analysis

Caspase-3 activity was measured using an ELISA kit (Uscn Life Science Inc. Wuhan.). The ELISA procedures were performed according to the manufacturer's instructions. The test principle applied in this kit was the Sandwich enzyme immunoassay. The microtiter plate provided in this kit was pre-coated with an antibody that is specific to caspase-3. Standards or samples were then added to the appropriate microtiter plate wells with a biotin-conjugated antibody specific to caspase-3. Next, avidin conjugated to Horseradish peroxidase (HRP) was added to each microplate well and incubated. After TMB (3, 3', 5, 5'-tetramethylbenzidine) substrate solution was added, only the wells that contained caspase-3, biotin-conjugated antibody and enzyme-conjugated avidin exhibited a change in color. The enzyme-substrate reaction was terminated by the addition of sulfuric acid solution, and the color change was measured spectrophotometrically at a wavelength of 450 nm (BioTek ELx800 Absorbance Microplate Reader). The results are expressed as ng/mg-protein.

2.3.2. Tissue tumor necrosis factor-alpha (TNF- α) analysis

The tissue TNF- α level was measured using the ELISA kit (Uscn Life Science Inc. Wuhan.). The test principle applied in this kit was the Sandwich enzyme immunoassay. The microtiter plate provided in this kit was pre-coated with an antibody specific to TNF- α . Standards or samples were then added to the appropriate microtiter plate wells with a biotin-conjugated antibody specific to TNF- α . Next, avidin conjugated to HRP was added to each microplate well and incubated. After TMB substrate solution was added, only the wells that contained TNF- α , biotin-conjugated antibody and enzyme-conjugated avidin exhibited a change in color. The enzyme-substrate reaction was terminated by the addition of sulfuric acid solution, and the color change was measured spectrophotometrically at a wavelength of 450 nm. The results are expressed as pg/mg.

2.3.3. Tissue myeloperoxidase (MPO) analysis

The MPO activity was measured using the ELISA kit (Uscn Life Science Inc. Wuhan.). The ELISA procedures were carried out according to the manufacturer's instructions. The test principle applied in this kit was the Sandwich enzyme immunoassay. The microtiter plate provided in this kit was pre-coated with an

antibody specific to MPO. Standards or samples were then added to the appropriate microtiter plate wells with a biotin-conjugated antibody specific to MPO. Next, avidin conjugated to HRP was added to each microplate well and incubated. After TMB substrate solution was added, only the wells that contained MPO, biotin-conjugated antibody and enzyme-conjugated avidin exhibited a change in color. The enzyme-substrate reaction was terminated by the addition of sulfuric acid solution, and the color change was measured spectrophotometrically at a wavelength of 450 nm. The results are expressed as pg/mg.

2.3.4. Tissue malondialdehyde (MDA) analysis

The tissue MDA levels were determined by a method based on the reaction with thiobarbituric acid (TBA) as described previously by Ohkawa et al. (1979). Briefly, 100 ml of tissue homogenate was added to 50 ml of sodium dodecyl sulfate (SDS, 8.1%), then this mixture was vortexed and incubated for 10 min at room temperature. Then, 375 μ l of acetic acid (pH 3.5, 20%) and 375 μ l of TBA (0.6%) were added to this solution, and the samples were heated in boiling water for 60 min. After cooling at room temperature, 1.25 ml of butanol:pyridine (15:1) was added to each test tube and vortexed. The mixture was centrifuged at 4000g for 5 min. The absorbance of the 750 μ l of the organic layer in 1 ml of cells was read at 532 nm. Malondialdehyde concentrations were expressed as nmol/mg-protein.

2.3.5. Tissue nitric oxide (NO) analysis

Tissue NO levels were determined using the method described by Miranda et al. (2001). Briefly, isolated tissues were homogenized in 10 ml of ice-cold saline solution and then absolute ethanol was added to precipitate the proteins. After allowing the materials to separate over a 15-min period (at 25 °C), the supernatant was recovered. To 0.5 ml of supernatant, 0.5 ml vanadium (III) chloride (8 mg VCl₃/ml) was added, rapidly followed by the addition of 0.5 ml freshly prepared Griess reagent (1% sulfanilamide, 2% phosphoric acid, and 0.1% N-1 naphthylethylene diamine dihydrochloride; 500 μ l). The mixture was then vortexed and incubated at 37 °C for 30 min before its absorbance was measured at 540 nm using the double-beam spectrophotometer. The results are expressed as nmol/mg protein.

2.3.6. Tissue superoxide dismutase (SOD) analysis

Total (Cu–Zn and Mn) SOD (EC 1.15.1.1) activity was determined according to the method described by Sun et al. (1988). The principle of the method is based on the inhibition of nitrobluetetrazolium reduction by the xanthine–xanthine oxidase system as a superoxide generator. Activity was assessed in the ethanol phase of the supernatant after 1.0 ml ethanol/chloroform mixture (5/3, v/v) was added to the same volume of sample and centrifuged. One unit of SOD was defined as the enzyme amount causing 50% inhibition of nitrobluetetrazolium reduction. Superoxide dismutase activity was expressed as U/mg-protein.

2.4. Histopathological procedures

The spinal cord tissues of all rats in all the groups were embedded in paraffin and fixed with 10% buffered formalin for 24 h. Using a microtome, 5 μ m-thick serial sections were cut from the paraffin blocks and stained with hematoxylin-eosin (H&E) for routine histopathological observations. All of the tissue sections were observed under a light microscope by a neuropathologist who was blinded to the study design.

A semiquantitative scoring system, ranging between zero and three, was used for grading both histopathological changes (edema, vascular congestion, and inflammation) and the neuronal

degenerative signs (nuclear pyknosis, nuclear hyperchromasia, cytoplasmic eosinophilia and axonal edema) in all of the spinal cord tissue samples. Four different histopathologically assessed parameters were scored as follows; 0: absent; 1: mild; 2: moderate; and 3: common. The pathological score for each spinal cord was calculated based on the sum of the scores of these four different parameters (Kertmen et al., 2013).

To assess the degree of neuronal injury in more detail, the number of normal motor neurons in the anterior horn of the spinal cord (anterior to a line drawn through the central canal perpendicular to the vertebral axis) was counted in 3 sections for each animal and then averaged.

2.5. Ultrastructural examination

Tissue samples were cleared of blood using a scalpel, and the meninges were carefully removed. The tissue samples were fixed in 2.5% glutaraldehyde for 24 h, washed in phosphate buffer (pH: 7.4), post-fixed in 1% osmium tetroxide in phosphate buffer (pH: 7.4) for 2 h and dehydrated in increasing concentrations of alcohol. Then, the tissues were washed with propylene oxide and embedded in epoxy-resin embedding media. Semi-thin sections of approximately 2 μ m in thickness and ultra thin sections of approximately 60 nm in thickness were cut with a glass knife on a LKB-Nova (LKB-Produkter AB, Bromma, Sweden) ultramicrotome. The semi-thin sections were stained with methylene blue and examined using a Nikon Optiphot (Nikon Corporation, Tokyo, Japan) light microscope. Following this examination, the tissue blocks were trimmed, their ultra thin sections were made using the same ultramicrotome and stained with uranyl acetate and lead citrate. Following staining, all the ultra thin sections were examined using a Jeol JEM 1200 EX (Jeol Ltd., Tokyo, Japan) transmission electron microscope. The electron micrographs were taken by the same transmission electron microscope. Every 100 large-diameter myelinated axons, medium-diameter myelinated axons, and small-diameter myelinated axons, evaluated and scored from 0 to 3 as described by Kaptanoglu et al. (2002).

The scoring system was as follows: 0: Ultrastructurally normal myelinated axon. 1: Separation in the myelin configuration. 2: Interruption in the myelin configuration. 3: Honeycomb appearance in the myelin configuration.

2.6. Neurological evaluation

Neurologic status of the animals was scored 24 h after the procedure based on assessment using the Basso, Beattie, and Bresnahan (BBB) locomotor scale and the inclined-plane test.

The open-field locomotor test assessed the movement, weight support, and coordination of the rats, and the results were scored using the BBB locomotor scale, where 0 indicates no motor activity and 21 indicates a normal performance (Basso et al., 1995). To summarize, animals were allowed to walk around freely in a circular field for 5 min, and the movements of the hind limbs were closely observed. The animals' ability to maintain postural stability was assessed with the inclined-plane test. The rats were placed on the inclined plane, and the maximum inclination at which the rat could maintain its position for 5 s was recorded as the final angle (Han et al., 2011). Two independent examiners who were blinded to the experimental protocols observed the rats during the tests.

2.7. Statistical analysis

Data analysis was performed using SPSS for Windows, version 11.5 (SPSS Inc., Chicago, IL, USA). Whether the continuous variables were normally distributed or not was determined using Shapiro Wilk test. Levene test was used for the evaluation of the homogeneity of the variances. Data are shown as the median (IQR). Whether the

differences in median values among groups were statistically significant was evaluated using Kruskal Wallis test. When the P values from Kruskal Wallis test statistics were statistically significant, Conover's non-parametric multiple comparison test was used to determine which group differed from the other group. The degrees of association between continuous variables were calculated using Spearman's Rank Correlation analyses. A P value less than 0.05 was considered statistically significant.

3. Results

3.1. Tissue caspase-3 activity

There were statistically significant differences among the tissue caspase-3 activity determined when the trauma group was compared both with the control and the sham groups ($P < 0.001$ for both). These data showed that SCI clearly caused an elevation of caspase-3 activity in the damaged tissue. When the ROS group was compared with the trauma group, there was a statistically significant decrease in caspase-3 activity ($P = 0.001$). As in the ROS group, the MP group also showed a statistically significant decrease in caspase-3 activity ($P = 0.019$). There was no significant difference between the control and the sham groups ($P = 0.929$) or between the MP and the ROS groups ($P = 0.811$).

3.2. Tissue tumor necrosis factor-alpha (TNF- α) levels

After SCI, tissue TNF- α levels were increased significantly when both the control and the sham groups were compared to the trauma group ($P = 0.002$ and $P < 0.001$, respectively). The administration of ROS significantly reduced tissue TNF- α levels compared to the trauma group ($P < 0.001$). Additionally, the administration of MP significantly reduced the tissue TNF- α levels compared with the trauma group ($P < 0.001$). No significant difference was observed between the control and the sham groups ($P = 0.058$) or between the MP and the ROS groups ($P = 0.612$).

3.3. Tissue myeloperoxidase (MPO) activity

When tissue MPO activities of the control and the sham groups were compared with the trauma group, a statistically significant difference was observed ($P < 0.001$ for both); these data showed that after SCI, tissue MPO activity was increased. Treatment with ROS significantly decreased the tissue MPO activity ($P = 0.026$). As in the ROS group, MP treatment also significantly decreased the

MPO activity in the spinal cord ($P = 0.04$). There was no significant difference between the control and the sham groups ($P = 0.905$) or between the MP and the ROS groups ($P = 0.858$).

3.4. Tissue malondialdehyde (MDA) levels

When mean tissue MDA levels of the control and the sham groups were compared with the trauma group, statistically significant differences were observed ($P < 0.001$ for both). So these data showed that after SCI, tissue MDA levels were increased. When we compared the trauma and the ROS groups, a statistically significant difference observed ($P < 0.001$). As in the ROS group, the comparison between the trauma and the MP groups revealed a statistically significant difference ($P = 0.004$). There was no significant difference between the control and the sham groups ($P = 0.698$) or between the MP and the ROS groups ($P = 0.357$).

3.5. Tissue nitric oxide (NO) levels

Tissue NO levels were found to be significantly increased in the trauma group when compared with both the control and the sham groups ($P < 0.001$ for both). In the ROS group, tissue NO levels were significantly decreased compared to the trauma group ($P < 0.001$). Similar to the ROS group, in the MP group, the NO levels were significantly decreased compared to the trauma group ($P = 0.001$). There was no significant difference between the control and the sham groups ($P = 0.12$) or between the MP and the ROS groups ($P = 0.512$).

3.6. Tissue superoxide dismutase (SOD) activity

Following SCI, tissue SOD activity decreased significantly when both the control and the sham groups were compared with the trauma group ($P < 0.001$ for both). Both treatment with ROS and MP significantly increased the tissue SOD activity compared to the trauma group ($P = 0.001$ and $P = 0.004$, respectively). There was no significant difference between the control and the sham groups ($P = 0.335$) or between the MP and the ROS groups ($P = 0.623$). The biochemical results of the study are shown in Table 1.

3.7. Histopathological procedures

Light microscopic examinations of the spinal cord samples from the control and the sham groups were normal (Fig. 1A and B). In the trauma group, diffuse hemorrhage and congestion in the gray

Table 1
Biochemical results relevant to the study groups.

| Variables | Control | Sham | Trauma | MP | ROS | P-value |
|----------------------------------|----------------------------------|----------------------------------|--------------------------------------|-----------------------------------|-----------------------------------|---------|
| Tissue caspase-3 (ng/mg-protein) | 155.4 (52.12) ^{a, b, c} | 136.0 (66.82) ^{d, e, f} | 790.7 (607.05) ^{a, d, g, h} | 420.6 (508.87) ^{b, e, g} | 415.7 (374.05) ^{c, f, h} | < 0.001 |
| Tissue TNF- α (pg/mg) | 23.0 (2.34) ^{a, c} | 19.8 (8.11) ^d | 39.5 (3.87) ^{a, d, g, h} | 20.0 (7.22) ^g | 19.8 (2.21) ^{c, h} | < 0.001 |
| Tissue MPO (pg/mg) | 133.4 (39.61) ^{a, b, c} | 134.9 (47.16) ^{d, e, f} | 296.5 (165.01) ^{a, b, c, f} | 235.5 (66.95) ^{b, e, g} | 220.8 (67.87) ^{c, f, h} | < 0.001 |
| Tissue MDA (nmol/mg-protein) | 1.05 (0.55) ^{a, b} | 0.93 (1.28) ^{d, e, f} | 4.39 (1.30) ^{a, d, g, h} | 1.67 (1.14) ^{b, e, g} | 1.47 (0.54) ^{f, h} | < 0.001 |
| Tissue NO (nmol/mg) | 47.3 (14.58) ^a | 37.2 (23.69) ^{d, e} | 90.6 (21.69) ^{a, d, g, h} | 53.8 (22.75) ^{e, g} | 48.9 (32.55) ^h | < 0.001 |
| Tissue SOD (U/mg) | 1.3 (0.05) ^{a, b, c} | 1.4 (0.12) ^{d, e, f} | 0.3 (0.11) ^{a, b, e, f} | 1.1 (0.44) ^{b, e, g} | 1.0 (0.36) ^{c, f, h} | < 0.001 |

MP: methylprednisolone, ROS: rosuvastatin, TNF- α : tumor necrosis factor-alpha, MPO: myeloperoxidase, MDA: malondialdehyde, NO: nitric oxide, SOD: superoxide dismutase.

^a Control vs. trauma ($P < 0.01$).

^b Control vs. MP ($P < 0.01$).

^c Control vs. ROS ($P < 0.05$).

^d Sham vs. trauma ($P < 0.001$).

^e Sham vs. MP ($P < 0.05$).

^f Sham vs. ROS ($P < 0.05$).

^g Trauma vs. MP ($P < 0.05$).

^h Trauma vs. ROS ($P < 0.05$).

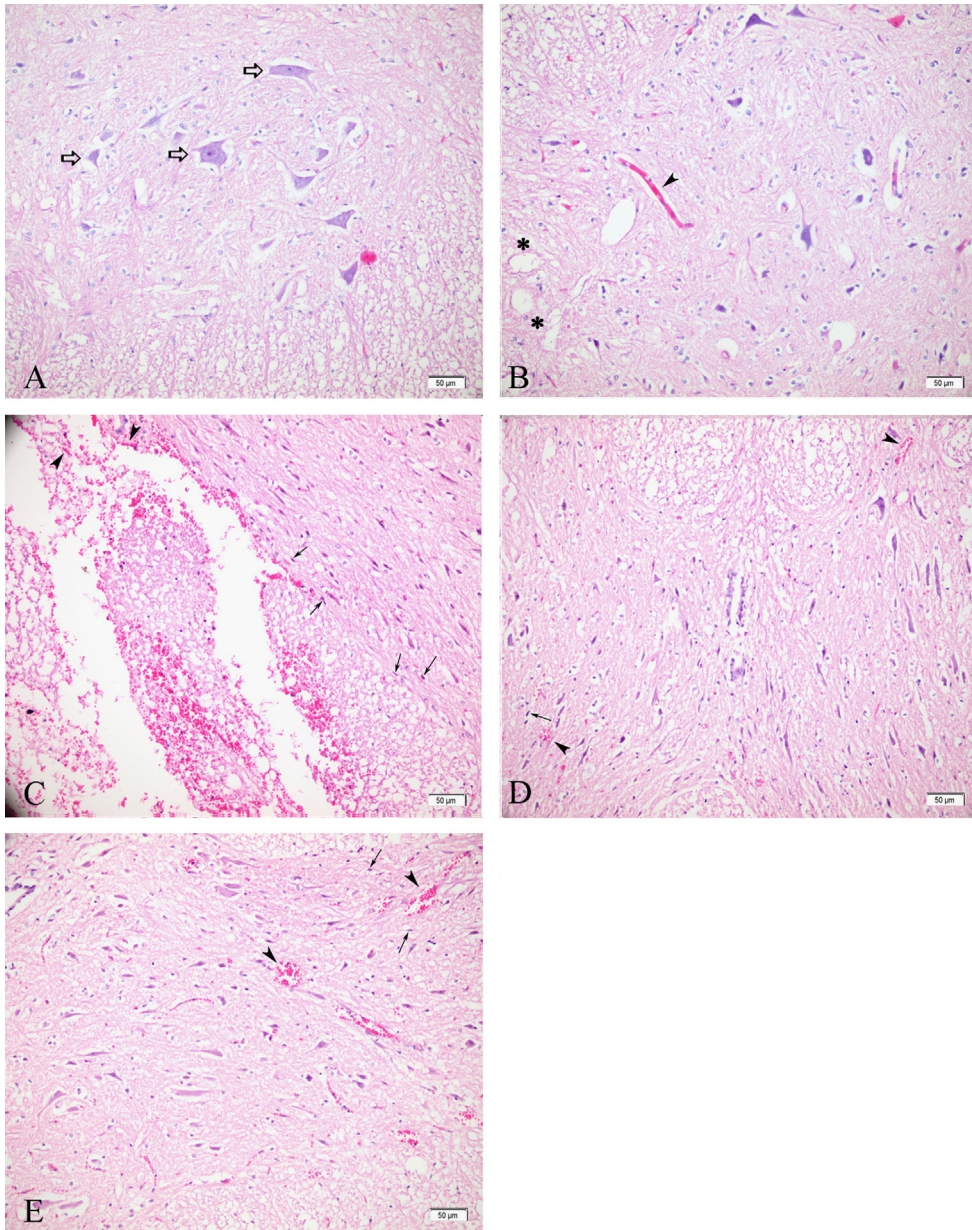


Fig. 1. Photomicrographs of 5- μ m-thick spinal cord tissue sections from the different treatment groups (H&E, X200). A. Control group, showing normal appearing spinal cord parenchyma and non-degenerated normal neurons (arrow). B. Sham group, showing normal appearing spinal cord parenchyma only with mild edema (*) and mild hemorrhagic congestion (arrow head). C. Trauma group, showing highly degenerated neurons (filled arrow). Spinal cord parenchyma is highly edematous and revealing hemorrhage and congestion (arrow head). D. Rosuvastatin group, showing less degenerated neurons (filled arrow), and more normal appearing neurons. The cord tissues were well protected from injury, revealing less edema and mild hemorrhagic congestion (arrow head). E. Methylprednisolone group, showing less degenerated neurons (filled arrow), less edema and mild hemorrhagic congestion (arrow head).

matter were observed at 24 h after SCI. There was marked necrosis and edema. Additionally, in the damaged portions, polymorphonuclear leukocyte, lymphocyte and plasma cell infiltration were observed. Neural pyknosis, a loss of cytoplasmic features, and cytoplasmic eosinophilia were observed in the trauma group (Fig. 1C). In the ROS group, as well as in the MP group, the spinal cord samples were well protected from SCI (Fig. 1D and E).

When the pathological scores were compared, the trauma group had statistically higher scores than both the control and the sham groups ($P < 0.001$ for both). In the ROS group, pathological score was significantly lower than the trauma group ($P < 0.001$). As expected, in the MP group, the pathology score was also significantly lower than the trauma group ($P = 0.042$).

There was no significant difference between the control and the sham groups ($P = 0.08$) or between the MP and the ROS groups ($P = 0.066$).

In the trauma group, the number of normal motor neurons in the anterior spinal cord was significantly decreased compared with both the control and the sham groups ($P < 0.001$ for both). In the ROS group, the number of normal motor neurons in the anterior spinal cord was significantly higher compared with the trauma group ($P = 0.003$). Similar to the ROS group, the MP group also showed significantly higher numbers of normal motor neurons compared with the trauma group ($P = 0.01$). The comparison between the ROS and the MP groups did not show any significant differences ($P = 0.687$). The histopathological results are shown in Table 2.

Table 2
Histopathological and electron microscopic results relevant to the study groups.

| Myelinated axon | Control | Sham | Trauma | MP | ROS | P-value |
|--------------------------------------|-----------------------------------|----------------------------------|-------------------------------------|-----------------------------------|-----------------------------------|---------|
| Pathology score | 2.0 (1.50) ^{a, b} | 0.0 (0.00) ^{c, d, e} | 9.5 (2.00) ^{a, c, f, g} | 5.5 (3.50) ^{b, d, f} | 3.0 (1.50) ^{e, g} | < 0.001 |
| Number of normal neurons | 46.0 (7.50) ^{a, b, h} | 44.5 (4.50) ^{c, d, e} | 21.0 (2.00) ^{a, c, f, g} | 34.5 (6.50) ^{b, d, f} | 35.5 (5.25) ^{e, g, h} | < 0.001 |
| Small-sized myelinated axons | 0.0 (0.00) ^{a, b, h} | 0.0 (0.00) ^{c, d, e} | 86.0 (6.00) ^{a, c, f, g} | 77.0 (7.00) ^{b, d, f, i} | 1.0 (2.00) ^{h, e, g, i} | < 0.001 |
| Medium-sized myelinated axons | 12.0 (3.50) ^{a, b, h, j} | 0.0 (0.00) ^{c, d, e, j} | 124.0 (18.50) ^{a, c, f, g} | 89.0 (4.00) ^{b, d, f, i} | 65.0 (4.00) ^{h, e, g, i} | < 0.001 |
| Large-sized myelinated axons | 16.0 (5.00) ^{a, b, h, j} | 4.0 (3.50) ^{c, d, e, j} | 140.0 (12.00) ^{a, c, f, g} | 98.0 (2.50) ^{b, d, f, i} | 78.0 (4.00) ^{h, e, g, i} | < 0.001 |

MP: methylprednisolone, ROS: rosvustatin.

^a Control vs. trauma ($P < 0.01$).

^b Control vs. MP ($P < 0.05$).

^c Sham vs. trauma ($P < 0.01$).

^d Sham vs. MP ($P < 0.01$).

^e Sham vs. ROS ($P < 0.05$).

^f Trauma vs. MP ($P < 0.05$).

^g Trauma vs. ROS ($P < 0.001$).

^h Control vs. ROS ($P < 0.05$).

ⁱ MP vs. ROS ($P < 0.01$).

^j Control vs. Sham ($P < 0.05$).

3.8. Ultrastructural examination

In the transmission electron microscopic examination of the tissue samples of the control group, ultrastructural pathological changes were not observed in the gray and white matters of the spinal cord. The neurons were ultrastructurally normal in appearance; the intracellular organelles, nuclei and membranes of the neurons were ultrastructurally normal. The perineuronal tissues did not show any pathological changes. However, only in a few of the large sized myelinated axons, mild separations were observed in a small part of the myelin sheath. This may be related to the delayed fixation of the tissue. The rest of the large sized myelinated axons and the whole medium- and small-sized myelinated axons were ultrastructurally normal (Fig. 2A).

In the ultrastructural examination of the sham group, no ultrastructural pathology was detected in the gray matter. In the ultrastructural examination of the white matter, mild separations in myelin configuration were observed in very few of the medium-sized and large-sized myelinated axons. Small sized myelinated axons were ultrastructurally normal (Fig. 2B).

In the transmission electron microscopic examination of the tissue samples of the trauma group, separations and interruptions in the myelin configuration were observed in the small-sized, medium-sized and large-sized myelinated axons. In the structural examination of the gray matter, swollen mitochondria and vacuoles were observed inside the cytoplasm of neurons. Additionally, perineuronal edema was observed (Fig. 2C).

In the ROS group, ultrastructural examination of the gray matter revealed dilatations in the perinuclear cisternae. Additionally, a small amount of perineuronal edema was present. In the ultrastructural examination of the white matter, mild separations in myelin configuration were observed in the medium-sized and large-sized myelinated axons. The small-sized axons were ultrastructurally normal. The ultrastructural appearances of the myelinated axons of this group were better than the MP group (Fig. 2D).

In the MP group, ultrastructural examination of the gray matter showed swollen mitochondria, and vacuoles were observed inside the cytoplasm of neurons. Additionally, perineuronal edema was present. In the ultrastructural examination of the white matter, separations in the myelin configuration were found in small-sized, medium-sized and large-sized myelinated axons (Fig. 2E).

When compared to the control and the sham groups, the trauma group showed more disruption in the small-sized myelinated axons ($P < 0.001$ for both). When compared to the trauma group, both the ROS and MP protected the small-sized myelinated axons from disruption ($P < 0.001$ and $P = 0.014$, respectively).

Furthermore, ROS protected the small-sized myelinated axons better than MP ($P < 0.001$).

In the trauma group, it was found that after SCI, the medium-sized myelinated axons were injured compared to both the control and the sham groups ($P < 0.001$ for both). There was a significant difference between both the ROS and the MP groups compared to the trauma group ($P < 0.001$ and $P = 0.014$, respectively); both the ROS and MP treatments protected medium-sized myelinated axons from traumatic SCI. Furthermore, when the ROS group was compared to the MP group, the ROS group revealed significantly better results in terms of protecting the medium-sized myelinated axons ($P = 0.008$).

Additionally, it was found that the large-sized myelinated axons were damaged after SCI when the trauma group was compared to both the control and the sham groups ($P < 0.001$ for both). Both the administration of ROS and MP protected large-sized myelinated axons compared to the trauma group ($P < 0.001$ and $P = 0.008$, respectively). Moreover, the ROS group revealed better results than the MP group ($P = 0.008$). The results of the ultrastructural examinations relevant to the study groups are shown in Table 2.

3.9. Neurologic evaluation

All the animals had an initial BBB score of 21. Following SCI, the mean BBB score of the trauma group was decreased statistically significantly compared with the control and the sham groups ($P < 0.001$ for both). Both the ROS and the MP groups showed better BBB scores compared to the trauma group ($P = 0.001$ and $P = 0.004$, respectively). There was no significant difference between the control and the sham groups ($P = 1$) or between the MP and the ROS groups ($P = 0.141$).

Following SCI, the mean angle recorded in the inclined-plane test was significantly lower in the trauma group than in the control and the sham groups ($P < 0.001$ for both). Both ROS and MP treatments revealed better angles in the inclined-plane test compared to the trauma group ($P = 0.002$ and $P = 0.001$, respectively). There was no significant difference between the control and the sham groups ($P = 0.058$) or between the MP and the ROS groups ($P = 0.493$). The results of the neurological examinations relevant to the study groups are shown in Table 3.

Furthermore, correlation analyses were performed among the variables. The pathology score and the number of normal neurons were positively correlated with caspase-3, TNF- α , MPO, MDA and NO levels and were negatively correlated with SOD activity. The ultrastructural results relevant to the small-sized, medium-sized

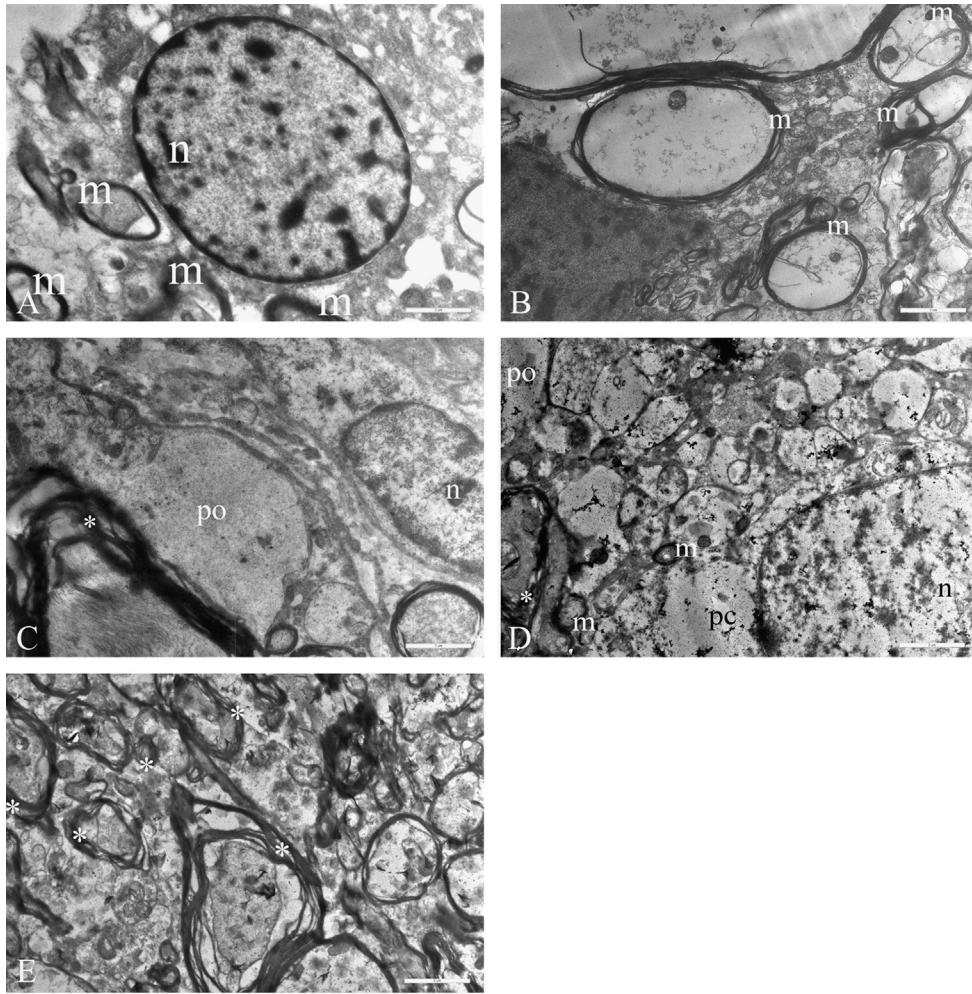


Fig. 2. Transmission electron microscopy of the groups. A. In the transmission electron microscopic examination of the tissue samples of the control group, ultrastructural pathological changes were not observed in the gray and white matters of the spinal cord. m: ultrastructurally normal myelinated axon; n: nucleus of a normal appearing neuron (Bar represents 2 μ m). B. Electron micrograph from the sham group revealed no ultrastructural pathology in the gray matter. In the white matter, mild separations in myelin configuration were observed in very few of the medium sized and large sized myelinated axons might be explained with delayed fixation. m: ultrastructurally normal myelinated axon (Bar represents 2 μ m). C. Electron micrograph from the trauma group showing perineural edema (po) and separation in myelin configuration (*) of a myelinated axon. n: nucleus of neuron (Bar represents 2 μ m). D. Electron micrograph from the rosuvastatin group showing mild perineural edema (po) and a myelinated axons with separation in myelin configuration (*), dilatations in perinuclear cisternae (pc), ultrastructurally normal myelinated axons (m), n: nucleus of neuron (Bar represents 2 μ m). E. Electron micrograph from the methylprednisolone group showing separations in myelin configuration (*) in medium and small sized myelinated axons (Bar represents 2 μ m).

Table 3

Neurological examination results relevant to the study groups.

| Variable | Control | Sham | Trauma | MP | ROS | P-value |
|--------------------------|--------------------------------|--------------------------------|-----------------------------------|---------------------------------|---------------------------------|---------|
| BBB score | 21.0 (0.00) ^{a, b, c} | 21.0 (0.00) ^{d, e, f} | 2.0 (0.75) ^{a, d, g, h} | 6.0 (1.50) ^{b, e, g} | 8.0 (1.00) ^{c, f, h} | < 0.001 |
| Inclined-plane angle (°) | 68.5 (6.25) ^{a, b, c} | 77.0 (7.00) ^{d, e, f} | 34.5 (4.25) ^{a, d, g, h} | 52.5 (10.50) ^{b, e, g} | 56.0 (13.25) ^{c, f, h} | < 0.001 |

MP: methylprednisolone, ROS: rosuvastatin, BBB: Basso, Beattie, and Bresnahan.

^a Control vs. trauma ($P < 0.001$).

^b Control vs. MP ($P < 0.01$).

^c Control vs. ROS ($P < 0.05$).

^d Sham vs. trauma ($P < 0.001$).

^e Sham vs. MP ($P < 0.001$).

^f Sham vs. ROS ($P < 0.01$).

^g Trauma vs. MP ($P < 0.05$).

^h Trauma vs. ROS ($P < 0.01$).

and large-sized myelinated axons were positively correlated with caspase-3, MPO, MDA and NO levels and negatively correlated with SOD activity. The BBB score and the inclined-plane angle

were negatively correlated with caspase-3, TNF- α , MPO, MDA and NO levels and positively correlated with SOD activity. The correlation analyses are shown in Table 4.

Table 4
The results of the correlation analyses.

| Variables | Caspase-3 activity | TNF- α levels | MPO activity | MDA levels | NO levels | SOD activity |
|---|--------------------|----------------------|----------------|----------------|----------------|----------------|
| Pathology score | | | | | | |
| Coefficient of correlation | 0.738 | 0.436 | 0.721 | 0.713 | 0.626 | -0.749 |
| P-value | < 0.001 | 0.005 | < 0.001 | < 0.001 | < 0.001 | < 0.001 |
| Number of normal neurons | | | | | | |
| Coefficient of correlation | -0.745 | -0.442 | -0.799 | -0.667 | -0.611 | 0.780 |
| P-value | < 0.001 | 0.004 | < 0.001 | < 0.001 | < 0.001 | < 0.001 |
| Small-sized myelinated axons | | | | | | |
| Coefficient of correlation | 0.749 | 0.309 | 0.598 | 0.768 | 0.593 | -0.889 |
| P-value | < 0.001 | 0.133 | 0.002 | < 0.001 | 0.002 | < 0.001 |
| Medium-sized myelinated axons | | | | | | |
| Coefficient of correlation | 0.749 | 0.254 | 0.744 | 0.762 | 0.650 | -0.873 |
| P-value | < 0.001 | 0.220 | < 0.001 | < 0.001 | < 0.001 | < 0.001 |
| Large-sized myelinated axons | | | | | | |
| Coefficient of correlation | 0.765 | 0.311 | 0.724 | 0.801 | 0.667 | -0.891 |
| P-value | < 0.001 | 0.130 | < 0.001 | < 0.001 | < 0.001 | < 0.001 |
| BBB score | | | | | | |
| Coefficient of correlation | -0.764 | -0.419 | -0.783 | -0.751 | -0.620 | 0.796 |
| P-value | < 0.001 | 0.007 | < 0.001 | < 0.001 | < 0.001 | < 0.001 |
| Inclined-plane angle ($^{\circ}$) | | | | | | |
| Coefficient of correlation | -0.693 | -0.468 | -0.772 | -0.743 | -0.608 | 0.837 |
| P-value | < 0.001 | 0.002 | < 0.001 | < 0.001 | < 0.001 | < 0.001 |

TNF- α : tumor necrosis factor-alpha, MPO: myeloperoxidase, MDA: malondialdehyde, NO: nitric oxide, SOD: superoxide dismutase, BBB: Basso, Beattie, and Bresnahan.

4. Discussion

Trauma to the spinal cord causes injury due to primary and secondary damage to the neuronal tissue. The most important secondary factors, which lead to further neuronal death, are apoptosis (Beattie et al., 2002; Chittenden et al., 1995), inflammation (Bartholdi and Schwab, 1995; Esposito et al., 2012; Kaltschmidt et al., 1993), lipid peroxidation (Dinc et al., 2013; Sonmez et al., 2013), and the development of reactive oxygen species (Hulsebosch, 2002; Vaziri et al., 2004).

Previous experimental studies have demonstrated the beneficial effects of statins in SCI (Déry et al., 2009; Esposito et al., 2012; Han et al., 2012, 2011; Mann et al., 2010; Pannu et al., 2007, 2005). As statins were shown to have neuroprotective effects on traumatic SCI, we studied the effects of ROS on SCI, which had not been previously studied. Rosuvastatin is a novel and a very potent statin (McKenney et al., 2003). Furthermore, there are two encouraging reasons to study ROS in SCI. First, ROS has a very rapid bioavailability because it does not require hepatic metabolism for activation (McKenney et al., 2003). This rapid bioavailability may cause a quick response to SCI. Secondly, ROS was thought to have superior neuroprotective effects compared to other statins (Zacco et al., 2003). The dosage of the ROS used in this study was based on pharmacological data from other rat studies where an oral dose of 12 mg/kg with an ED₅₀ of 0.8 mg/kg completely inhibits cholesterol synthesis (McTaggart et al., 2001). Additionally, other previous neuroprotection studies relevant to ROS suggested the dose used in the present study (Jungner et al., 2013; Kilic et al., 2005; Sironi et al., 2003).

To date, recommended treatments for SCI involve the administration of high-dose MP. MP is the only neuroprotective drug that achieved widespread adoption, although the efficiency and safety of MP has been intensely questioned, leading to discontinuation of its use in some settings (Hurlbert and Hamilton, 2008). As MP is widely used in the experimental models of SCI, we compared the results of ROS with MP (Schröter et al., 2009; Yin et al., 2013).

Neuronal death following SCI may due to necrosis (Balentine, 1978; Borgens et al., 1986) or apoptosis (Crowe et al., 1997; Liu et al., 1997). Apoptosis causes death of neuronal cells, especially

neurons and oligodendrocytes in the spinal cord after trauma, further disrupts and destroys the axon-myelin structural unit and impairs impulse conduction, resulting in neuronal loss (Crowe et al., 1997; Pannu et al., 2005). Caspase-3 is an interleukin converting enzyme and has been implicated as the principal effector of apoptosis in mammalian cells (Keane et al., 2001). Therefore, caspase-3 is a reliable marker for indicating apoptotic activity (Sakurai et al., 2003). The antiapoptotic effects of statins had been previously reported (Déry et al., 2009; Pannu et al., 2005; Tapia-Pérez et al., 2010), and the mechanism of prevention of apoptosis was thought to be modulation of caspase-3 (Déry et al., 2009). In this study, we showed that after trauma, caspase-3 activity increased significantly as an indicator of apoptosis. Both ROS and MP treatments prevented apoptosis in the spinal cord by inhibiting caspase-3 activity.

Inflammatory reactions play an important role in traumatic secondary injury after SCI (Bartholdi and Schwab, 1995; Hayashi et al., 2000; Hsu and Dimitrijevic, 1990). Within a few hours after experimental SCI, proinflammatory cytokines, such as TNF- α , are upregulated (Bartholdi and Schwab, 1995; Hayashi et al., 2000). Upregulated TNF- α levels were shown to mediate inflammation that causes secondary tissue damage and apoptosis after SCI (Pan et al., 2003). Furthermore, TNF- α plays an important role in neurodegeneration due to its early production after SCI (Hayashi et al., 2000; Lee et al., 2000). Our data revealed that following SCI, TNF- α levels were significantly increased. Both ROS and MP treatments showed anti-inflammatory effects by inhibiting TNF- α levels.

Following SCI, the neutrophils and other phagocytes reach the injured spinal cord tissue and produce hypochlorite, a strong oxidant synthesized by the enzyme MPO (Bao et al., 2004). Myeloperoxidase activity is strongly correlated with the absolute number of neutrophils and their inflammatory activity in the injured area (Christie et al., 2008; Mullane et al., 1985). In the present study, following SCI, the mean MPO activity was increased. Both ROS and MP administration caused a significant decrease in MPO activity, revealing the anti-inflammatory effects of both drugs.

Oxidative stress following SCI produces free radicals and initiates lipid peroxidation activity in the damaged neural tissue

(Torres et al., 2010). In our study, spinal cord levels of MDA, which are stable products of lipid peroxidation, increased significantly after traumatic SCI. Both ROS and MP administration decreased the levels of MDA by inhibiting lipid peroxidation. Similarly, Ucak et al. (2011) reported that ROS decreased the MDA levels as a marker of reduced oxidative stress after spinal cord ischemia-reperfusion injury in rats.

Oxidative stress is accompanied by antioxidant depletion and excess production of oxygen free radicals and NO at the site of injury (Vaziri et al., 2004). Oxygen free radicals can cause cytotoxicity by damaging lipids, proteins and nucleic acids (Dawson et al., 1994). Furthermore, oxidative stress plays a major part in the progression of spinal cord lesions after the primary injury (Hulsebosch, 2002). Neuronal tissues such as the spinal cord are highly vulnerable to oxidative injury because the central nervous system consists largely of lipids. Statins may also be neuroprotective through potential antioxidant effects (Delanty et al., 2001). The oxygen radical, NO, functions as a signaling molecule in the vascular system. In addition, overproduction of NO leads to oxidative damage (Moro et al., 2004). Previous studies demonstrated that statins reduce NO overproduction by reducing inducible nitric oxide synthetase (van der Most et al., 2009). However, due to elevated oxidative stress in the spinal cord, SOD levels were shown to decrease (Yilmaz et al., 2013). In this study, we also demonstrated that after traumatic SCI, NO levels were increased and SOD levels were decreased due to highly elevated oxidative stress in the spinal cord. On the other hand, ROS and MP treatments decreased the NO levels and increased the antioxidant enzyme SOD levels in the traumatized tissue. This is thought to be evidence for the antioxidant effect of ROS.

Histopathological examination of the spinal cord samples revealed that trauma to the spinal cord caused diffuse hemorrhage, marked edema, and necrosis. However, in the damaged portions of the spinal cord, there were infiltrating polymorphonuclear leukocytes, lymphocytes and plasma cells, which indicates an inflammatory response. Additionally, in the trauma group, normal motor neurons in the anterior spinal cord were significantly decreased in number. Both the ROS and the MP groups showed better morphological results and a high number of normal motor neurons compared with the trauma group. Furthermore, ROS produced better histomorphological results than MP.

Nevertheless, the evaluation of the neuroprotection using histological techniques under a light microscope does not always provide adequate conclusions; therefore, we also evaluated the ultrastructural changes under transmission electron microscope. All small-, medium- and large-sized myelinated axons were significantly disturbed after traumatic SCI. Rosuvastatin protected the spinal cord from traumatic injury by preserving the small-, medium- and large-sized myelinated axons. However, methylprednisolone also produced the same protective effects, but ROS showed better ultrastructural results than MP.

Despite the lack of a significant difference between ROS and MP for each of the biochemical parameters, ROS produced better histopathological and ultrastructural results than MP. We hypothesized that this conflict occurred because there were only a few biochemical parameters studied in this study, so ROS had further neuroprotective activity through other biochemical pathways than were investigated in this study.

The functional efficiency of the treatment was evaluated by locomotor performance with BBB scores (Basso et al., 1995). All rats had a BBB score of 21/21 before the trauma, and the traumatic SCI caused a significant decrease in BBB scores within 24 h. Rosuvastatin and MP treatments both revealed better BBB scores compared to the trauma group. Additionally, the mean angle in the inclined-plane test was decreased following the traumatic SCI. As expected, both ROS and MP increased the mean angle in the

inclined-plane test. As a result of these functional tests, both ROS and MP treatments following SCI protected the spinal cord and improved neurological functions.

All the results of this study suggest that ROS have beneficial effects on preserving normal spinal cord morphology, ultrastructure and function by inhibiting apoptosis, reducing inflammation and oxidative stress.

However, this study has some limitations. The number of rats in each group may be modified to produce stronger conclusions. The dose dependent results may be investigated. Delayed biochemical and histopathological assessment may provide better results for further studies. Furthermore, comparing rosuvastatin with other statins that has been reported previously to treat SCI such as simvastatin and atorvastatin is important. This comparison may provide a more comprehensive confirmation about the superior efficacy of rosuvastatin over the other statins.

5. Conclusions

In conclusion, the biochemical, histopathological, ultrastructural analyses and the functional tests revealed that ROS exhibits meaningful neuroprotective effects over SCI through antiapoptotic, anti-inflammatory, and antioxidant effects by reducing lipid peroxidation. The results of our study provided the first experimental evidence of the neuroprotective effects of ROS in traumatic SCI. Therefore, in light of these results, we believe that ROS may be a potential neuroprotective agent for clinical trials of SCI.

References

- Balentine, J.D., 1978. Pathology of experimental spinal cord trauma. I. The necrotic lesion as a function of vascular injury. *Lab. Invest.* 39, 236–253.
- Bao, F., Chen, Y., Dekaban, G.A., Weaver, L.C., 2004. Early anti-inflammatory treatment reduces lipid peroxidation and protein nitration after spinal cord injury in rats. *J. Neurochem.* 88, 1335–1344.
- Bartholdi, D., Schwab, M.E., 1995. Methylprednisolone inhibits early inflammatory processes but not ischemic cell death after experimental spinal cord lesion in the rat. *Brain Res.* 672, 177–186.
- Basso, D.M., Beattie, M.S., Bresnahan, J.C., 1995. A sensitive and reliable locomotor rating scale for open field testing in rats. *J. Neurotrauma* 12, 1–21.
- Beattie, M.S., Hermann, G.E., Rogers, R.C., Bresnahan, J.C., 2002. Cell death in models of spinal cord injury. *Prog. Brain Res.* 137, 37–47.
- Blight, A.R., 1992. Macrophages and inflammatory damage in spinal cord injury. *J. Neurotrauma* 9 (Suppl 1), S83–S91.
- Borgens, R.B., Blight, A.R., Murphy, D.J., 1986. Axonal regeneration in spinal cord injury: a perspective and new technique. *J. Comp. Neurol.* 250, 157–167.
- Cemil, B., Topuz, K., Demircan, M.N., Kurt, G., Tun, K., Kutlay, M., Ipcioglu, O., Kucukodaci, Z., 2010. Curcumin improves early functional results after experimental spinal cord injury. *Acta Neurochir.* 152, 1583–1590.
- Chittenden, T., Harrington, E.A., O'Connor, R., Flemington, C., Lutz, R.J., Evan, G.I., Guild, B.C., 1995. Induction of apoptosis by the Bcl-2 homologue Bak. *Nature* 374, 733–736.
- Christie, S.D., Comeau, B., Myers, T., Sadi, D., Purdy, M., Mendez, I., 2008. Duration of lipid peroxidation after acute spinal cord injury in rats and the effect of methylprednisolone. *Neurosurg. Focus* 25, E5.
- Crowe, M.J., Bresnahan, J.C., Shuman, S.L., Masters, J.N., Beattie, M.S., 1997. Apoptosis and delayed degeneration after spinal cord injury in rats and monkeys. *Nat. Med.* 3, 73–76.
- Dawson, T.M., Dawson, V.L., Snyder, S.H., 1994. Molecular mechanisms of nitric oxide actions in the brain. *Ann. N. Y. Acad. Sci.* 738, 76–85.
- Delanty, N., Vaughan, C.J., Sheehy, N., 2001. Statins and neuroprotection. *Expert Opin. Investig. Drugs* 10, 1847–1853.
- Déry, M.A., Rousseau, G., Benderdour, M., Beaumont, E., 2009. Atorvastatin prevents early apoptosis after thoracic spinal cord contusion injury and promotes locomotion recovery. *Neurosci. Lett.* 453, 73–76.
- Die, J., Wang, K., Fan, L., Jiang, Y., Shi, Z., 2010. Rosuvastatin preconditioning provides neuroprotection against spinal cord ischemia in rats through modulating nitric oxide synthase expressions. *Brain Res.* 1346, 251–261.
- Dinc, C., Iplikcioglu, A.C., Atabey, C., Eroglu, A., Topuz, K., Ipcioglu, O., Demirel, D., 2013. Comparison of deferoxamine and methylprednisolone: protective effect of pharmacological agents on lipid peroxidation in spinal cord injury in rats. *Spine* 38, E1649–E1655.
- Domoki, F., Kis, B., Gáspár, T., Snipes, J.A., Bari, F., Busija, D.W., 2010. Rosuvastatin induces delayed preconditioning against l-glutamate excitotoxicity in cultured cortical neurons. *Neurochem. Int.* 56, 404–409.

- Dumont, R.J., Okonkwo, D.O., Verma, S., Hurlbert, R.J., Boulos, P.T., Ellegala, D.B., Dumont, A.S., 2001. Acute spinal cord injury, part I: pathophysiologic mechanisms. *Clin. Neuropharmacol.* 24, 254–264.
- Esposito, E., Rinaldi, B., Mazzone, E., Donniacuo, M., Impellizzeri, D., Paterniti, I., Capuano, A., Bramanti, P., Cuzzocrea, S., 2012. Anti-inflammatory effect of simvastatin in an experimental model of spinal cord trauma: involvement of PPAR- α . *J. Neuroinflamm.* 9, 81.
- Fletcher, B., Berra, K., Aedes, P., Braun, L.T., Burke, L.E., Durstine, J.L., Fair, J.M., Fletcher, G.F., Goff, D., Hayman, L.L., Hiatt, W.R., Miller, N.H., Krauss, R., Kris-Etherton, P., Stone, N., Wilterdink, J., Winston, M., 2005. Managing abnormal blood lipids: a collaborative approach. *Circulation* 112, 3184–3209.
- Han, X., Yang, N., Cui, Y., Xu, Y., Dang, G., Song, C., 2012. Simvastatin mobilizes bone marrow stromal cells migrating to injured areas and promotes functional recovery after spinal cord injury in the rat. *Neurosci. Lett.* 521, 136–141.
- Han, X., Yang, N., Xu, Y., Zhu, J., Chen, Z., Liu, Z., Dang, G., Song, C., 2011. Simvastatin treatment improves functional recovery after experimental spinal cord injury by upregulating the expression of BDNF and GDNF. *Neurosci. Lett.* 487, 255–259.
- Hayashi, M., Ueyama, T., Nemoto, K., Tamaki, T., Senba, E., 2000. Sequential mRNA expression for immediate early genes, cytokines, and neurotrophins in spinal cord injury. *J. Neurotrauma* 17, 203–218.
- Hsu, C.Y., Dimitrijevic, M.R., 1990. Methylprednisolone in spinal cord injury: the possible mechanism of action. *J. Neurotrauma* 7, 115–119.
- Hulsebosch, C.E., 2002. Recent advances in pathophysiology and treatment of spinal cord injury. *Adv. Physiol. Educ.* 26, 238–255.
- Hurlbert, R.J., Hamilton, M.G., 2008. Methylprednisolone for acute spinal cord injury: 5-year practice reversal. *Can. J. Neurol. Sci.* 35, 41–45.
- Indraswari, F., Wang, H., Lei, B., James, M.L., Kernagis, D., Warner, D.S., Dawson, H.N., Laskowitz, D.T., 2012. Statins improve outcome in murine models of intracranial hemorrhage and traumatic brain injury: a translational approach. *J. Neurotrauma* 29, 1388–1400.
- Jungner, M., Lundblad, C., Bentzer, P., 2013. Rosuvastatin in experimental brain trauma: improved capillary patency but no effect on edema or cerebral blood flow. *Microvasc. Res.* 88, 48–55.
- Kaltschmidt, B., Baeuerle, P.A., Kaltschmidt, C., 1993. Potential involvement of the transcription factor NF- κ B in neurological disorders. *Mol. Aspects Med.* 14, 171–190.
- Kaptanoglu, E., Palaoglu, S., Surucu, H.S., Hayran, M., Beskonakli, E., 2002. Ultrastructural scoring of graded acute spinal cord injury in the rat. *J. Neurosurg.* 97 (1 Suppl.), S49–S56.
- Keane, R.W., Kraydieh, S., Lotocki, G., Bethea, J.R., Krajewski, S., Reed, J.C., Dietrich, W.D., 2001. Apoptotic and anti-apoptotic mechanisms following spinal cord injury. *J. Neuropathol. Exp. Neurol.* 60, 422–429.
- Kertmen, H., Güler, B., Yilmaz, E.R., Sanli, A.M., Sorar, M., Arıkkök, A.T., Sargon, M.F., Kanat, M.A., Ergüder, B.I., Sekerci, Z., 2013. The protective effect of low-dose methotrexate on ischemia-reperfusion injury of the rabbit spinal cord. *Eur. J. Pharmacol.* 714, 148–156.
- Kilic, U., Bassetti, C.L., Kilic, E., Xing, H., Wang, Z., Hermann, D.M., 2005. Post-ischemic delivery of the 3-hydroxy-3-methylglutaryl coenzyme A reductase inhibitor rosuvastatin protects against focal cerebral ischemia in mice via inhibition of extracellular-regulated kinase-1/2. *Neuroscience* 134, 901–906.
- Kurt, G., Ergün, E., Cemil, B., Börcek, A.O., Börcek, P., Gülbahar, O., Ceviker, N., 2009. Neuroprotective effects of infliximab in experimental spinal cord injury. *Surg. Neurol.* 71, 332–336.
- Laufs, U., Gertz, K., Dirnagl, U., Böhm, M., Nickenig, G., Endres, M., 2002. Rosuvastatin, a new HMG-CoA reductase inhibitor, upregulates endothelial nitric oxide synthase and protects from ischemic stroke in mice. *Brain Res.* 942, 23–30.
- Lee, Y.B., Yune, T.Y., Baik, S.Y., Shin, Y.H., Du, S., Rhim, H., Lee, E.B., Kim, Y.C., Shin, M.L., Markelonis, G.J., Oh, T.H., 2000. Role of tumor necrosis factor- α in neuronal and glial apoptosis after spinal cord injury. *Exp. Neurol.* 166, 190–195.
- Liu, X.Z., Xu, X.M., Hu, R., Du, C., Zhang, S.X., McDonald, J.W., Dong, H.X., Wu, Y.J., Fan, G.S., Jacquin, M.F., Hsu, C.Y., Choi, D.W., 1997. Neuronal and glial apoptosis after traumatic spinal cord injury. *J. Neurosci.* 17, 5395–5406.
- Mann, C.M., Lee, J.H., Hillyer, J., Stammers, A.M., Tetzlaff, W., Kwon, B.K., 2010. Lack of robust neurologic benefits with simvastatin or atorvastatin treatment after acute thoracic spinal cord contusion injury. *Exp. Neurol.* 221, 285–295.
- Mautes, A.E., Weinzierl, M.R., Donovan, F., Noble, L.J., 2000. Vascular events after spinal cord injury: contribution to secondary pathogenesis. *Phys. Ther.* 80, 673–687.
- McKenney, J.M., Jones, P.H., Adamczyk, M.A., Cain, V.A., Bryzinski, B.S., Blasetto, J.W., 2003. Comparison of the efficacy of rosuvastatin versus atorvastatin, simvastatin, and pravastatin in achieving lipid goals: results from the STELLAR trial. *Curr. Med. Res. Opin.* 19, 689–698.
- McTaggart, F., Buckett, L., Davidson, R., Holdgate, G., McCormick, A., Schneck, D., Smith, G., Warwick, M., 2001. Preclinical and clinical pharmacology of Rosuvastatin, a new 3-hydroxy-3-methylglutaryl coenzyme A reductase inhibitor. *Am. J. Cardiol.* 87, 28B–32B.
- Miranda, K.M., Espey, M.G., Wink, D.A., 2001. A rapid, simple spectrophotometric method for simultaneous detection of nitrate and nitrite. *Nitric Oxide* 5, 62–71.
- Moro, M.A., Cárdenas, A., Hurtado, O., Leza, J.C., Lizasoain, I., 2004. Role of nitric oxide after brain ischaemia. *Cell Calcium* 36, 265–275.
- Mullane, K.M., Kraemer, R., Smith, B., 1985. Myeloperoxidase activity as a quantitative assessment of neutrophil infiltration into ischemic myocardium. *J. Pharmacol. Methods* 14, 157–167.
- Ohkawa, H., Ohishi, N., Yagi, K., 1979. Assay for lipid peroxides in animal tissues by thiobarbituric acid reaction. *Anal. Biochem.* 95, 351–358.
- Pan, W., Zhang, L., Liao, J., Csernus, B., Kastin, A.J., 2003. Selective increase in TNF alpha permeation across the blood-spinal cord barrier after SCI. *J. Neuroimmunol.* 134, 111–117.
- Pannu, R., Barbosa, E., Singh, A.K., Singh, I., 2005. Attenuation of acute inflammatory response by atorvastatin after spinal cord injury in rats. *J. Neurosci. Res.* 79, 340–350.
- Pannu, R., Christie, D.K., Barbosa, E., Singh, I., Singh, A.K., 2007. Post-trauma Lipitor treatment prevents endothelial dysfunction, facilitates neuroprotection, and promotes locomotor recovery following spinal cord injury. *J. Neurochem.* 101, 182–200.
- Prinz, V., Laufs, U., Gertz, K., Kronenberg, G., Balkaya, M., Leithner, C., Lindauer, U., Endres, M., 2008. Intravenous rosuvastatin for acute stroke treatment: an animal study. *Stroke* 39, 433–438.
- Sakurai, M., Nagata, T., Abe, K., Horinouchi, T., Itoyama, Y., Tabayashi, K., 2003. Survival and death-promoting events after transient spinal cord ischemia in rabbits: induction of Akt and caspase3 in motor neurons. *J. Thorac. Cardiovasc. Surg.* 125, 370–377.
- Sánchez-Aguilar, M., Tapia-Pérez, J.H., Sánchez-Rodríguez, J.J., Viñas-Ríos, J.M., Martínez-Pérez, P., de la Cruz-Mendoza, E., Sánchez-Reyna, M., Torres-Corzo, J.G., Gordillo-Moscote, A., 2013. Effect of rosuvastatin on cytokines after traumatic head injury. *J. Neurosurg.* 118, 669–675.
- Savoia, C., Sisalli, M.J., Di Renzo, G., Annunziato, L., Scorziello, A., 2011. Rosuvastatin-induced neuroprotection in cortical neurons exposed to OGD/reoxygenation is due to nitric oxide inhibition and ERK1/2 pathway activation. *Int. J. Physiol. Pathophysiol. Pharmacol.* 3, 57–64.
- Schröter, A., Lustenberger, R.M., Obermair, F.J., Thallmair, M., 2009. High-dose corticosteroids after spinal cord injury reduce neural progenitor cell proliferation. *Neuroscience* 161, 753–763.
- Sironi, L., Cimino, M., Guerrini, U., Calvio, A.M., Lodetti, B., Asdente, M., Balduini, W., Paoletti, R., Tremoli, E., 2003. Treatment with statins after induction of focal ischemia in rats reduces the extent of brain damage. *Arterioscler. Thromb. Vasc. Biol.* 23, 322–327.
- Sonmez, E., Kabatas, S., Ozen, O., Karabay, G., Turkoglu, S., Ogun, E., Yilmaz, C., Caner, H., Altınor, N., 2013. Minocycline treatment inhibits lipid peroxidation, preserves spinal cord ultrastructure, and improves functional outcome after traumatic spinal cord injury in the rat. *Spine* 38, 1253–1259.
- Stepień, K., Tomaszewski, M., Czuczwar, S.J., 2005. Neuroprotective properties of statins. *Pharmacol. Rep.* 57, 561–569.
- Sun, Y., Oberley, L.W., Li, Y., 1988. A simple method for clinical assay of superoxide dismutase. *Clin. Chem.* 34, 497–500.
- Tapia-Pérez, J.H., Sánchez-Aguilar, M., Schneider, T., 2010. The role of statins in neurosurgery. *Neurosurg. Rev.* 33, 259–270.
- Torres, S., Salgado-Ceballos, H., Torres, J.L., Orozco-Suarez, S., Díaz-Ruiz, A., Martínez, A., Rivera-Cruz, M., Ríos, C., Lara, A., Collado, C., Guizar-Sahagún, G., 2010. Early metabolic reactivation versus antioxidant therapy after a traumatic spinal cord injury in adult rats. *Neuropathology* 30, 36–43.
- Ucak, A., Onan, B., Güler, A., Sahin, M.A., Kılıçkaya, O., Oztaş, E., Uysal, B., Arslan, S., Yilmaz, A.T., 2011. Rosuvastatin, a new generation 3-hydroxy-3-methylglutaryl coenzyme A reductase inhibitor, reduces ischemia/reperfusion-induced spinal cord tissue injury in rats. *Ann. Vasc. Surg.* 25, 686–695.
- van der Most, P.J., Dolga, A.M., Nijholt, I.M., Luiten, P.G., Eisel, U.L., 2009. Statins: mechanisms of neuroprotection. *Prog. Neurobiol.* 88, 64–75.
- Vaughan, C.J., Delanty, N., 1999. Neuroprotective properties of statins in cerebral ischemia and stroke. *Stroke* 30, 1969–1973.
- Vaziri, N.D., Lee, Y.S., Lin, C.Y., Lin, V.W., Sindhu, R.K., 2004. NAD(P)H oxidase, superoxide dismutase, catalase, glutathione peroxidase and nitric oxide synthase expression in subacute spinal cord injury. *Brain Res.* 995, 76–83.
- Yavuz, C., Demirtas, S., Guclu, O., Karahan, O., Caliskan, A., Yazici, S., Mavitas, B., 2013. Rosuvastatin may have neuroprotective effect on spinal cord ischemia reperfusion injury. *CNS. Neurol. Disord. Drug Targets* 12, 1011–1016.
- Yilmaz, E.R., Kertmen, H., Güler, B., Kanat, M.A., Arıkkök, A.T., Ergüder, B.I., Hasturk, A.E., Ergil, J., Sekerci, Z., 2013. The protective effect of 2-mercaptoethane sulfonate (MESNA) against traumatic brain injury in rats. *Acta Neurochir.* 155, 141–149.
- Yin, Y., Sun, W., Li, Z., Zhang, B., Cui, H., Deng, L., Xie, P., Xiang, J., Zou, J., 2013. Effects of combining methylprednisolone with rilpivirine on functional recovery in adult rats following spinal cord injury. *Neurochem. Int.* 62, 903–912.
- Zacco, A., Togo, J., Spence, K., Ellis, A., Lloyd, D., Furlong, S., Piser, T., 2003. 3-hydroxy-3-methylglutaryl coenzyme A reductase inhibitors protect cortical neurons from excitotoxicity. *J. Neurosci.* 23, 11104–11111.